

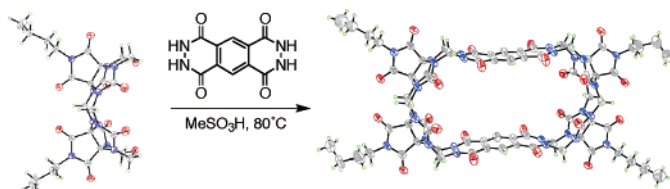
## Cucurbit[*n*]uril Analogues: Synthetic and Mechanistic Studies

Jason Lagona, James C. Fettinger, and Lyle Isaacs\*

Department of Chemistry and Biochemistry, University of Maryland, College Park, Maryland 20742

*lisaacs@umd.edu*

Received August 6, 2005



The synthesis of cucurbit[*n*]uril analogues (**18**, **19**, ( $\pm$ )-**20**, **33**, **34**, **35**, **36**, and **37**) is presented. These CB[5], CB[6], and CB[7] analogues all contain bis(phthalhydrazide) walls that are incorporated into the macrocycle. The tailor-made synthesis of these CB[*n*] analogues proceeds by the condensation of the appropriate bis(electrophile) (**4**, **7**, or **9**) with bis(phthalhydrazide) (**17**), which delivers the CB[6] and CB[7] analogues in good yield, whereas the CB[5] analogue is formed in low yield. To improve the solubility characteristics of the CB[*n*] analogues for recognition studies in water or organic solution, the CO<sub>2</sub>Et groups were transformed to CO<sub>2</sub>H and CO<sub>2</sub>(CH<sub>2</sub>)<sub>9</sub>CH<sub>3</sub> groups. On the basis of the results of product resubmission experiments, we conclude that these macrocycles are kinetic products. To help rationalize the good yields obtained in the CB[6] and CB[7] analogue macrocyclization reactions, we performed mechanistic studies of model methylene bridged glycoluril dimers, which suggest an intramolecular isomerization during CB[*n*] analogue formation.

### Introduction

CB[6] is a macrocyclic cavitand comprising six glycoluril units linked through 12 methylene bridges, which defines a hydrophobic cavity guarded by two carbonyl fringed portals. The unusual recognition properties of CB[6] have been delineated by the pioneering work of Mock,<sup>1</sup> Buschmann,<sup>2</sup> and Kim.<sup>3</sup> CB[6] has the ability to encapsulate guests in its hydrophobic cavity as the result of a combination of noncovalent interactions including the hydrophobic effect, ion–dipole interactions, and hydrogen bonding. The high selectivity exhibited by CB[6] is due to the relative rigidity of the macrocycle, which allows for guests of an appropriate size, shape, and chemical functionality to bind tightly. The formation of these CB[6]·guest complexes is easily detected by <sup>1</sup>H NMR, UV–vis, and isothermal titration calorimetry. In this paper, we incorporate fluorescent bis(phthalhydrazide) walls into CB[*n*] analogues, which allows the sensitive detection ( $K_a > 10^6 \text{ M}^{-1}$ ) of host–guest com-

plexation by fluorescence titrations.<sup>4,5</sup> The outstanding recognition properties of the CB[*n*] family<sup>6</sup> has resulted in numerous intriguing applications including molecular switches,<sup>7</sup> catalysis,<sup>8–11</sup> water purification in textile industries,<sup>12</sup> polyrotaxanes,<sup>13</sup> ion channels,<sup>14</sup> self-assem-

(4) Wagner, B. D.; Boland, P. G.; Lagona, J.; Isaacs, L. *J. Phys. Chem. B* **2005**, *109*, 7686–7691.

(5) Sindelar, V.; Cejas, M. A.; Raymo, F. M.; Kaifer, A. E. *New J. Chem.* **2005**, *29*, 280–282.

(6) Lagona, J.; Mukhopadhyay, P.; Chakrabarti, S.; Isaacs, L. *Angew. Chem., Int. Ed.* **2005**, *44*, 4844–4870.

(7) Mock, W. L.; Pierpont, J. *J. Chem. Soc., Chem. Commun.* **1990**, 1509–1511.

(8) Mock, W. L.; Irra, T. A.; Wepsiec, J. P.; Manimaran, T. L. *J. Org. Chem.* **1983**, *48*, 3619–3620; Tuncel, D.; Steinke, J. H. G. *Macromolecules* **2004**, *37*, 288–302. Pattabiraman, M.; Natarajan, A.; Kaanumalle, L. S.; Ramamurthy, V. *Org. Lett.* **2005**, *7*, 529–532.

(9) Mock, W. L.; Irra, T. A.; Wepsiec, J. P.; Adhya, M. *J. Org. Chem.* **1989**, *54*, 5302–5308.

(10) Jon, S. Y.; Ko, Y. H.; Park, S. H.; Kim, H.-J.; Kim, K. *Chem. Commun.* **2001**, 1938–1939.

(11) Choi, S.; Park, S. H.; Ziganshina, A. Y.; Ko, Y. H.; Lee, J. W.; Kim, K. *Chem. Commun.* **2003**, 2176–2177.

(12) Buschmann, H. J.; Schollmeyer, E. *Textilveredlung* **1998**, *33*, 44–47.

(13) Kim, K.; Kim, D.; Lee, J. W.; Ko, Y. H.; Kim, K. *Chem. Commun.* **2004**, 848–849; Meschke, C.; Buschmann, H. J.; Schollmeyer, E. *Macromol. Rapid Commun.* **1998**, *19*, 59–63. Tuncel, D.; Steinke, J. H. G. *Chem. Commun.* **2001**, 253–254.

(14) Jeon, J. J.; Kim, H.; Jon, S.; Selvapalam, N.; Oh, D. H.; Seo, I.; Park, C.-S.; Jung, S. R.; Koh, D.-K.; Kim, K. *J. Am. Chem. Soc.* **2004**, *126*, 15944–15945.

(1) Mock, W. L. *Top. Curr. Chem.* **1995**, *175*, 1–24.  
 (2) Hoffmann, R.; Knoche, W.; Fenn, C.; Buschmann, H.-J. *J. Chem. Soc., Faraday Trans.* **1994**, *90*, 1507–1511.  
 (3) Lee, J. W.; Samal, S.; Selvapalam, N.; Kim, H.-J.; Kim, K. *Acc. Chem. Res.* **2003**, *36*, 621–630. Kim, K. *Chem. Soc. Rev.* **2002**, *31*, 96–107.

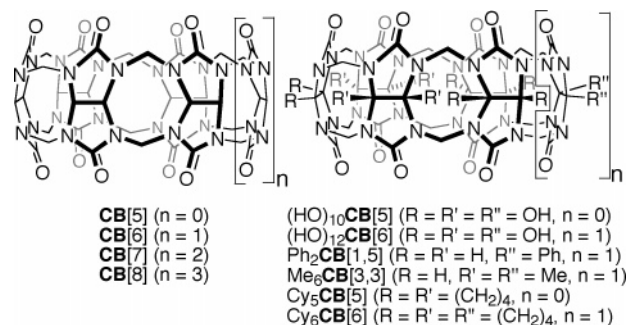
bling dendrimers,<sup>15</sup> as components of molecular machines,<sup>16</sup> and advanced separations technologies.<sup>17</sup>

When we began our work in this area, the range of applications to which CB[6] could be applied was limited by a series of issues: (1) poor solubility in aqueous and organic solution, (2) the lack of synthetic procedures to allow the preparation of CB[6] homologues, CB[*n*] derivatives, and CB[*n*] analogues,<sup>18</sup> and (3) the inability to change the binding selectivity of the macrocycles by incorporation of groups that define the cavity. In the intervening time, several of these issues have been alleviated either partially or fully. For example, when the condensation reaction was performed under milder conditions, CB[5], CB[7], CB[8], and CB[10] were isolated along with CB[6] as the major product.<sup>19,20</sup> The improved solubility of CB[7] and the spacious cavity of CB[8] gave rise to new opportunities in supramolecular chemistry.<sup>10,11,21</sup>

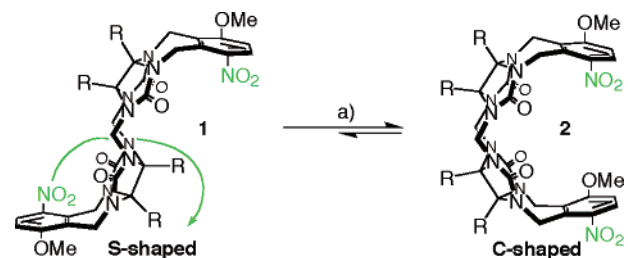
Two approaches have been reported for the preparation of CB[*n*] derivatives with enhanced solubility in water and organic solvents. The first involves the condensation of glycoluril derivatives, either alone or in combination with glycoluril, with formaldehyde under acidic conditions. This approach has resulted in the synthesis of several persubstituted CB[*n*] derivatives including Cy<sub>5</sub>-CB[5] and Cy<sub>6</sub>CB[6],<sup>22</sup> as well as the partially substituted CB[*n*] derivatives Ph<sub>2</sub>CB[1,5]<sup>23</sup> and Me<sub>6</sub>CB[3,3].<sup>24</sup> In pioneering work, Kim recently demonstrated a second approach, the direct functionalization of CB[*n*], which delivered perhydroxylated CB[*n*] derivatives including (HO)<sub>10</sub>CB[5] and (HO)<sub>12</sub>CB[6].<sup>25</sup>

Our approach to the synthesis of CB[*n*] derivatives and analogues relied on the identification of the methylene bridged glycoluril dimer structure (Chart 1, emboldened) as the fundamental building blocks of the CB[*n*] family. Our studies have focused, therefore, on methods for the preparation and interconversion of methylene bridged glycoluril dimers. We discovered that suitable combinations of nucleophilic and electrophilic glycoluril building blocks result in the selective formation of heterodimers

### CHART 1. CB[*n*] Homologues and Derivatives



### SCHEME 1. S- to C-Shaped Isomerization Reaction (*R* = CO<sub>2</sub>Et)<sup>a</sup>



<sup>a</sup> Conditions: (a) PTSA, (CICH<sub>2</sub>)<sub>2</sub>, reflux.

as a mixture of S-shaped and C-shaped diastereomers.<sup>26,27</sup> To rationalize the selective formation of C-shaped heterodimers, we studied the mechanism of the interconversion of **1** and **2**. We discovered that the S-shaped to C-shaped isomerization was an intramolecular process that occurs with retention of configuration (Scheme 1). The implications of these studies toward CB[*n*] synthesis were manifold. For example, we hypothesized that suitable combinations of glycoluril N–H compounds (e.g., **3**) and glycoluril bis(cyclic ethers) (e.g., **4**) would deliver control over size, shape, and functionalization pattern in CB[*n*]-forming reactions. Herein, we present a full report on the preparation of functionalized CB[*n*] analogues<sup>18</sup> with solubility in aqueous solutions and organic solvents through a tailor-made approach, as well as mechanistic studies that lead to insights on the stability and formation pathways of CB[*n*] analogues. These new CB[*n*] analogues are potentially useful in applications such as fluorescence-based sensors,<sup>4,5,28</sup> catalysis,<sup>9,10</sup> cation and molecular transport,<sup>14</sup> in self-sorting systems,<sup>29</sup> and as components of molecular machines.<sup>30</sup>

## Results and Discussion

**Oligomerization Reactions.** To access a series of bis(cyclic ether) electrophilic building blocks to test our

(15) Moon, K.; Grindstaff, J.; Sobransingh, D.; Kaifer, A. E. *Angew. Chem., Int. Ed.* **2004**, *43*, 5496–5499.

(16) Day, A. I.; Blanch, R. J.; Arnold, A. P.; Lorenzo, S.; Lewis, G. R.; Dance, I. *Angew. Chem., Int. Ed.* **2002**, *41*, 275–277. Marquez, C.; Hudgins, R. R.; Nau, W. M. *J. Am. Chem. Soc.* **2004**, *126*, 5808–5816.

(17) Liu, S.-M.; Xu, L.; Wu, C.-T.; Feng, Y.-Q. *Talanta* **2004**, *64*, 929–934. Wei, F.; Liu, S.; Xu, L.; Wu, C.; Feng, Y. *Sepu* **2004**, *22*, 476–478.

(18) Lagona, J.; Fettingner, J. C.; Isaacs, L. *Org. Lett.* **2003**, *5*, 3745–3747.

(19) Kim, J.; Jung, I.-S.; Kim, S.-Y.; Lee, E.; Kang, J.-K.; Sakamoto, S.; Yamaguchi, K.; Kim, K. *J. Am. Chem. Soc.* **2000**, *122*, 540–541.

(20) Day, A. I.; Arnold, A. P.; Blanch, R. J.; Snushall, B. *J. Org. Chem.* **2001**, *66*, 8094–8100.

(21) Blanch, R. J.; Sleeman, A. J.; White, T. J.; Arnold, A. P.; Day, A. I. *Nano Lett.* **2002**, *2*, 147–149. Ong, W.; Gomez-Kaifer, M.; Kaifer, A. E. *Org. Lett.* **2002**, *4*, 1791–1794. Wagner, B. D.; Stojanovic, N.; Day, A. I.; Blanch, R. J. *J. Phys. Chem. B* **2003**, *107*, 10741–10746. Ong, W.; Kaifer, A. E. *J. Org. Chem.* **2004**, *69*, 1383–1385; Moon, K.; Kaifer, A. E. *Org. Lett.* **2004**, *6*, 185–188.

(22) Zhao, J.; Kim, H.-J.; Oh, J.; Kim, S.-Y.; Lee, J. W.; Sakamoto, S.; Yamaguchi, K.; Kim, K. *Angew. Chem., Int. Ed.* **2001**, *40*, 4233–4235.

(23) Isobe, H.; Sato, S.; Nakamura, E. *Org. Lett.* **2002**, *4*, 1287–1289.

(24) Day, A. I.; Arnold, A. P.; Blanch, R. J. *Molecules* **2003**, *8*, 74–84.

(25) Jon, S. Y.; Selvapalam, N.; Oh, D. H.; Kang, J.-K.; Kim, S.-Y.; Jeon, Y. J.; Lee, J. W.; Kim, K. *J. Am. Chem. Soc.* **2003**, *125*, 10186–10187.

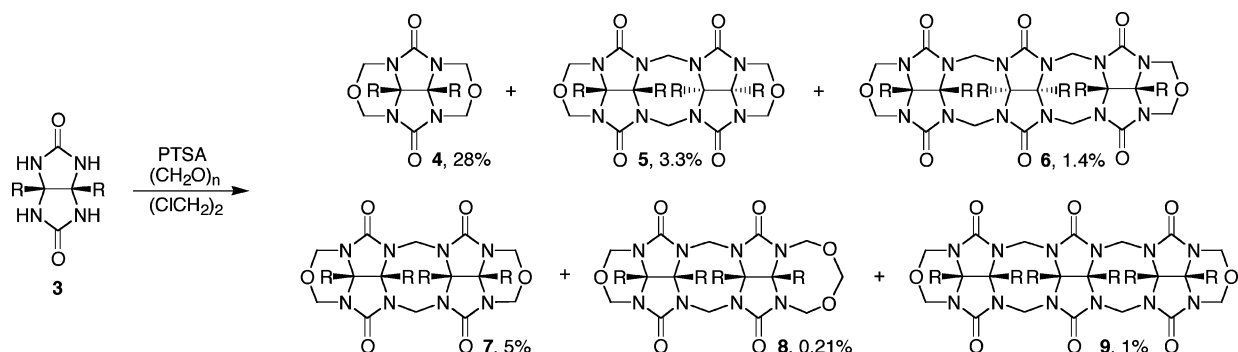
(26) Chakraborty, A.; Wu, A.; Witt, D.; Lagona, J.; Fettingner, J. C.; Isaacs, L. *J. Am. Chem. Soc.* **2002**, *124*, 8297–8306.

(27) Wu, A.; Chakraborty, A.; Witt, D.; Lagona, J.; Damkaci, F.; Ofori, M. A.; Chiles, J. K.; Fettingner, J. C.; Isaacs, L. *J. Org. Chem.* **2002**, *67*, 5817–5830.

(28) Marquez, C.; Huang, F.; Nau, W. M. *IEEE Trans. Nanobiosci.* **2004**, *3*, 39–45.

(29) Wu, A.; Chakraborty, A.; Fettingner, J. C.; Flowers, R. A.; Isaacs, L. *Angew. Chem., Int. Ed.* **2002**, *41*, 4028–4031. Wu, A.; Isaacs, L. *J. Am. Chem. Soc.* **2003**, *125*, 4831–4835. Mukhopadhyay, P.; Wu, A.; Isaacs, L. *J. Org. Chem.* **2004**, *69*, 6157–6164.

(30) Ko, Y. H.; Kim, K.; Kang, J.-K.; Chun, H.; Lee, J. W.; Sakamoto, S.; Yamaguchi, K.; Fettingner, J. C.; Kim, K. *J. Am. Chem. Soc.* **2004**, *126*, 1932–1933.

SCHEME 2. Controlled Oligomerization of **3** (R = CO<sub>2</sub>Et)

mechanistically guided hypotheses, we performed the condensation of **3** with paraformaldehyde in 1,2-dichloroethane in the presence of *p*-toluenesulfonic acid (PTSA) for 2 h at reflux. The bis(cyclic ether) monomer **4** was isolated as the major product along with oligomeric bis(cyclic ethers) (**5–9**) (Scheme 2). These compounds could be readily separated by column chromatography, and their structures were elucidated by <sup>1</sup>H NMR spectroscopy.<sup>18</sup>

We also confirmed our spectroscopic assignment of the structure of **5** and **7** by X-ray crystallography (Figure 1).

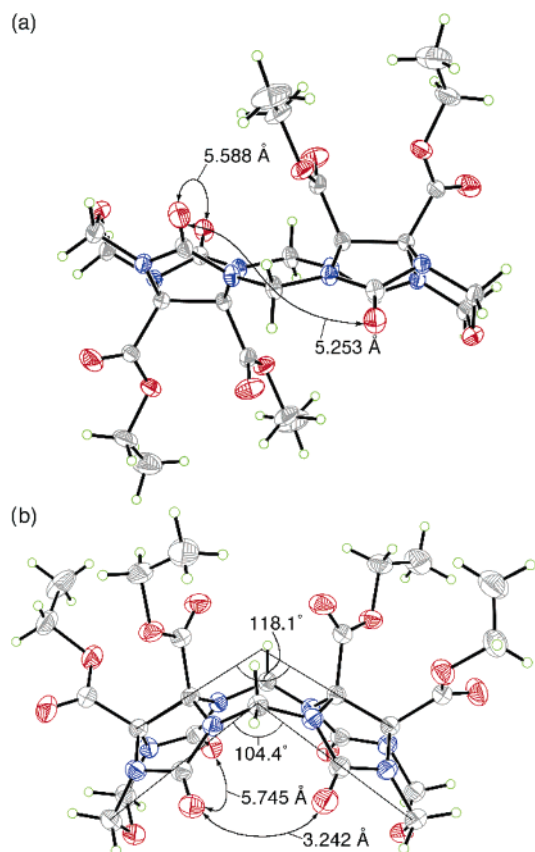


**FIGURE 1.** ORTEP plots of the X-ray crystal structures of (a) **5** and (b) **7** with 50% probability ellipsoids and selected distances and angles. Solvent molecules have been omitted for clarity. Color coding: C, gray; H, green; N, blue; O, red.

The X-ray structure of **5** establishes the relative configuration of the glycolurils rings that gives the S-shape to the molecule. This S-shaped stereochemistry between the

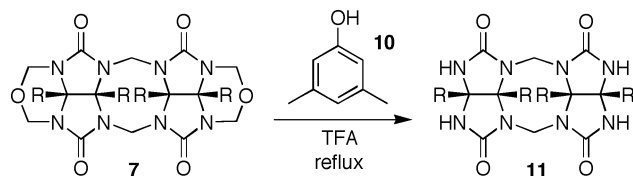
two glycoluril rings is not conducive to forming macrocyclic CB[*n*] derivatives or analogues unless isomerization to the C-shape occurs concomitantly. Compound **7** possesses a C-shape, which can be seen in the X-ray crystal structure. The glycoluril rings display both sets of R groups (CO<sub>2</sub>Et) on the same face of the molecule, which gives the molecule a curvature that promotes the formation of macrocycles. From Figure 1, it is evident that the O...O distances from the carbonyls in the same glycoluril are relatively similar for **5** and **7**, but the O...O distances for the carbonyls in the adjacent glycolurils differ by about 2 Å, which can be explained by the directionality incorporated into the shape of glycoluril. When the oligomer is in the S-shape (**5**), the carbonyls on the adjacent glycolurils point in opposite directions, whereas in the oligomer in the C-shape (**7**), the carbonyls on the adjacent glycolurils point in the same direction and begin to define the C=O portals characteristic of the CB[*n*] family.

With C-shaped electrophilic bis(cyclic ether) building blocks **4** and **7** in hand we set out to synthesize new CB[*n*] derivatives and analogues. We investigated the macrocyclization of the building blocks under a variety of conditions including refluxing bis(cyclic ethers) (**4**, **7**, or **9**) alone or a combination of bis(cyclic ethers) (**4** and **7**, **7** and **9**) in (ClCH<sub>2</sub>)<sub>2</sub> with PTSA for 1 day or longer at different bis(cyclic ether) and PTSA concentrations.<sup>31</sup> We also investigated the condensation of **3** with **4**, **3** with **7**, and **3** with **9** in hopes of isolating new CB[*n*] derivatives.<sup>24,32</sup> Unfortunately, we did not detect any macrocyclic compounds in these reactions. We hypothesize that the anhydrous acidic conditions employed to avoid potential saponification of the CO<sub>2</sub>Et groups slows down the S- to C-shaped isomerization of trimeric and higher oligomers, which results in oligomer formation rather than macrocyclization.<sup>20,26</sup>

**Heterocyclization.** To circumvent the problem of oligomerization of **4**, **7**, and **9**, we resorted to the synthesis of a nucleophilic dimer that could undergo heterodimerization with the bis(cyclic ether) building blocks. For this purpose, we heated **7** with 3,5-dimethylphenol (**10**) in CF<sub>3</sub>CO<sub>2</sub>H, which gave **11** in 63% yield (Scheme 3). We chose **10** as the reagent in this deprotection reaction because the *meta*-positions on the aromatic ring are

(31) The formation of macrocycles using bis(cyclic ethers) **4**, **7**, or **9** alone requires the formal extrusion of formaldehyde. Since there is an excess of methylene groups present in **4**, **7**, and **9** the formation of CB[*n*] might be disfavored under these conditions.

(32) Zhao, Y.; Xue, S.; Zhu, Q.; Tao, Z.; Zhang, J.; Wei, Z.; Long, L.; Hu, M.; Xiao, H.; Day, A. I. *Chin. Sci. Bull.* **2004**, *49*, 1111–1116.

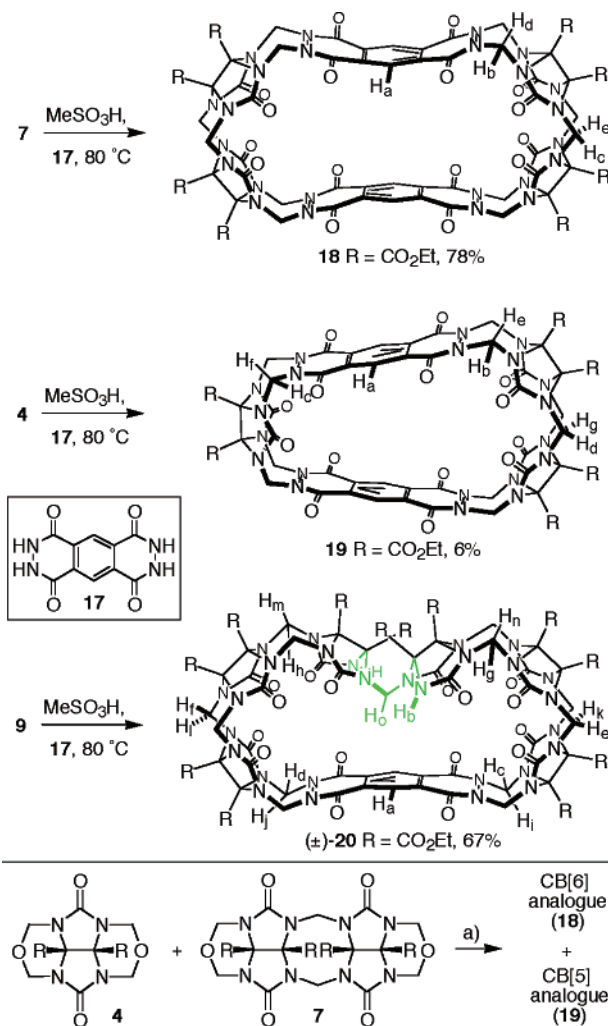
**SCHEME 3. Bis(cyclic ether) Deprotection (R = CO<sub>2</sub>Et, 63%)**

blocked, which prevents seven-membered ring formation and promotes removal of the CH<sub>2</sub> bridges from **7**.<sup>33</sup> Compound **11** has the same curvature as **7** but now possesses four potentially nucleophilic ureidyl N–H groups that can be used to form new methylene bridges in the synthesis of CB[*n*]. Our initial hypothesis was that the reaction between **7** and **11** under anhydrous acidic conditions would yield CB[*n*] with multiples of two (CB[6], CB[8], CB[10], etc.) glycoluril rings by a heterocyclization process that could be monitored by <sup>1</sup>H NMR analysis.<sup>34</sup> Unfortunately, we consistently observed either oligomerization or decomposition. As a result of our inability to use either **7** or **11** in the tailor-made synthesis of CB[*n*] derivatives with enhanced properties, we decided to search for other nucleophilic partners that might undergo selective heterodimerization reactions with the bis(cyclic ether) building blocks to ultimately deliver CB[*n*] analogues.

**Glycoluril Surrogates.** Through serendipity, we discovered that **12** and **13** undergo rapid, highly selective heterodimerization yielding **14** in 69% yield (Scheme 4). We attribute this result to the enhanced nucleophilicity of the hydrazide N–H groups present in **13** due to the α-effect. After obtaining this result, we were interested in studying the reactivity of other hydrazides. For example, condensation of **15** with **12** in TFA gave **16** in 55% yield (Scheme 4). We were able to perform this condensation reaction in TFA because of the increased solubility of **15**. Interestingly, if **16** is submitted to PTSA/(CICH<sub>2</sub>)<sub>2</sub> at reflux with 1 equiv of **13**, a replacement reaction is observed that delivers **14** in 81% yield. This result indicates that **13** is a superior partner in these reactions, presumably because it sacrifices less resonance energy upon condensation and suggests that CH<sub>2</sub>-bridges between glycoluril and phthalhydrazide rings form reversibly.

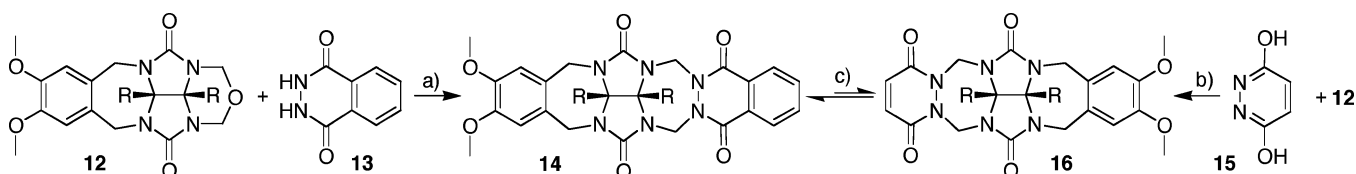
**CB[*n*] Analogues. Synthesis.** To allow for potential macrocycle formation, we synthesized bis(phthalhydrazide) **17** by the reaction of pyromellitic anhydride with hydrazine in acetic acid at reflux.<sup>35</sup> Compound **17**, which is planar, does not result in S- and C-shaped diastereomers upon reaction with **7**, which is expected to favor macrocyclization relative to oligomerization. Unfortunately, the solubility of **17** is poor in all common organic solvents (<1 mg/mL in CHCl<sub>3</sub>, CH<sub>3</sub>CN, (CICH<sub>2</sub>)<sub>2</sub>, PhH,

and TFA). After much experimentation, we found that **17** is soluble in hot, anhydrous MeSO<sub>3</sub>H.<sup>36</sup> Accordingly, we attempted the condensation reaction of **7** with **17** (Scheme 5). We were delighted to observe a remarkably

**SCHEME 5. Synthesis of CB[*n*] Analogues (R = CO<sub>2</sub>Et)<sup>a</sup>**

<sup>a</sup> Conditions: (a) **17**, MeSO<sub>3</sub>H, 80 °C

clean <sup>1</sup>H NMR spectrum of the crude reaction mixture. Pure CB[6] analogue **18** could be obtained in 78% yield simply by washing the crude solid with H<sub>2</sub>O and acetone. Next, we condensed the monomeric building block (**4**) with **17** to give the CB[5] analogue **19** although in much lower isolated yield (6%). Finally, we investigated the condensation of **9** with **17** in hope of forming a CB[8] analogue by a four-component macrocyclization. Once again, the crude reaction mixture was remarkably clean

**SCHEME 4. Glycoluril Surrogates 13 and 15<sup>a</sup>**

<sup>a</sup> Conditions: (a) PTSA, (CICH<sub>2</sub>)<sub>2</sub>, reflux, 69%; (b) TFA, reflux, 55%; (c) 1 equiv of **13**, PTSA, (CICH<sub>2</sub>)<sub>2</sub>, reflux, 81%. R = CO<sub>2</sub>Et

and we were able to isolate a single compound by SiO<sub>2</sub> chromatography in 67% yield.<sup>37</sup> Surprisingly, however, the new compound proved to be CB[7] analogue (±)-**20** formed by the condensation of 2 equiv of **9** with 1 equiv of **17**. This new macrocycle possesses several unusual structural features: (1) it is chiral and racemic as a result of its C<sub>2</sub>-symmetry, (2) it contains a single methylene bridge between the 2 equiv of **9**, and (3) this methylene group is directed into the cavity of (±)-**20**.

To understand the reasons behind the low yield obtained for CB[5] **19**, we carried out the three-component macrocyclization (**4** + **7** + **17**) shown in Scheme 5. In contrast to the low yield obtained with **4** and **17**, analysis of the crude <sup>1</sup>H NMR spectrum for the three-component macrocyclization indicated the clean formation of a 1:1 mixture of **18** and **19** in high yield. Unfortunately, we were unable to separate this mixture into its components. Apparently, the need to form methylene bridges *between glycolurils*, a process that is quite slow relative to the formation of methylene bridges between glycoluril and phthalhydrazide rings, in the macrocyclization of **4** and **17** alone is obviated by the use of **4**, **7**, and **17**. Consequently, a larger fraction of material undergoes macrocyclization rather than oligomerization in the three-component reaction. Although we were delighted with the formation of CB[5], CB[6], and CB[7] analogues (**18**–**20**), we were disappointed by their relatively low solubility in both aqueous and organic solvents. Whereas TFA and DMSO are excellent solvents for the CO<sub>2</sub>Et substituted CB[*n*] analogues, their solubilities in CH<sub>3</sub>CN were only modest (1–2 mM).

**<sup>1</sup>H NMR Spectral Characterization.** The <sup>1</sup>H NMR spectra of **18**, **19**, and **20** are shown in Figure 2 using the labeling from Scheme 5. The spectrum for **18** has the fewest resonances for the methylene protons as a result of its D<sub>2h</sub>-symmetry (Figure 2a). The diastereotopic protons H<sub>b</sub> and H<sub>d</sub> are on the methylene bridges connecting the bis(phthalhydrazide) and the glycoluril. The diastereotopic protons H<sub>c</sub> and H<sub>e</sub> resonate at chemical shifts similar to those of CB[*n*] methylene bridges because they are between the adjacent glycolurils. In contrast, the spectrum for C<sub>2v</sub>-symmetric macrocycle **19** has resonances for two pairs of diastereotopic protons between glycoluril and phthalhydrazide rings (H<sub>b</sub>, H<sub>c</sub>, H<sub>e</sub>, and H<sub>f</sub>, Figure 2b). The doublets for H<sub>d</sub> and H<sub>g</sub> appear at similar chemical shifts relative to macrocycle **18** corresponding to the methylene bridges that connect the two glycolurils. Finally, the <sup>1</sup>H NMR spectrum of mac-

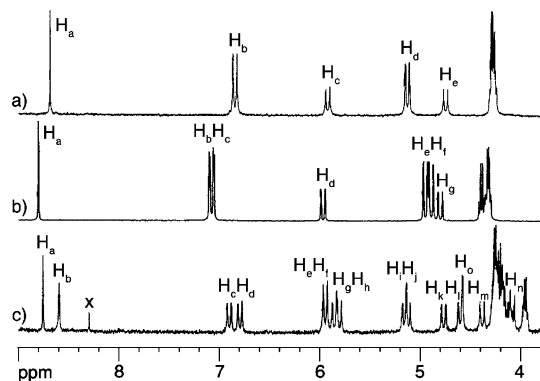


**FIGURE 2.** Portion of the <sup>1</sup>H NMR spectra (298 K, 400 MHz) recorded for (a) **18** in DMSO-*d*<sub>6</sub>, (b) **19** in CD<sub>3</sub>CN, (c) (±)-**20** in DMSO-*d*<sub>6</sub>. × = CHCl<sub>3</sub> in DMSO-*d*<sub>6</sub>. The unlabeled resonances come from the CO<sub>2</sub>CH<sub>2</sub>CH<sub>3</sub> groups.

rocycle (±)-**20**, which possesses a C<sub>2</sub> axis, gives rise to 12 doublets, some of which are overlapping (Figure 2c). Most notable is the resonance for proton H<sub>o</sub>, which appears as a singlet in the <sup>1</sup>H NMR spectrum because the methylene bridge connecting the two glycolurils (shown in green in Scheme 5) is similar to an S-shaped oligomer (**5**), making these protons magnetically equivalent.

**Synthesis of Glycoluril Building Blocks Designed to Enhance the Solubility of CB[*n*] Analogues.** To enhance the solubility of the CB[*n*] analogues in aqueous and organic media, we attempted both deprotection and transesterification of the ethyl esters on the equator of macrocycles **18**–**20**. Unfortunately, the phthalhydrazide linkages of **18**, **19**, and (±)-**20** are sensitive to base and these reactions were not successful. Accordingly, we decided to transform the CO<sub>2</sub>Et groups into carboxylic acid derivatives (e.g., amides, imides, esters, and acids) prior to macrocyclization (Scheme 6).<sup>38</sup>

For potential recognition studies in H<sub>2</sub>O, we performed the saponification of **4** and **7** with LiOH in CH<sub>3</sub>OH/H<sub>2</sub>O and were able to isolate the carboxylic acids **21** and **22** in 76% and 89% yield, respectively. To increase the solubility of the corresponding CB[*n*] analogues in organic media, we converted the CO<sub>2</sub>Et groups to different esters, amides, and imides by straightforward functional group manipulations.<sup>38</sup> For example, amidation reactions occurred smoothly by subjecting **4** and **7** to neat butylamine, delivering **23** in 90% and **24** in 68% yield, respectively. Compounds **23** and **24** could be converted to the imides **25** and **26** in 82 and 39% yield, respectively, by heating under anhydrous acidic conditions (PTSA/C(CH<sub>2</sub>)<sub>2</sub>, reflux). For highest solubility in organic solvents such as CHCl<sub>3</sub> and CH<sub>2</sub>Cl<sub>2</sub> we performed transesterification reactions to increase the lipophilicity of the building blocks, which renders the resulting CB[*n*] analogues soluble in nonpolar solvents. For this purpose, we selected the conditions used by Sanders for thermodynamically controlled transesterification reactions because this procedure was well established, provided good yields, and was simple to perform.<sup>39</sup> Accordingly, compound **7** was treated with 1-octadecyl alcohol to yield **27**

(33) The function of 3,5-dimethylphenol (**10**) in the reaction illustrated in Scheme 3 is to act as a formaldehyde scavenger. The CH<sub>2</sub> group of the bis(cyclic ether) portion of **7** is transferred to the aromatic ring through an electrophilic aromatic substitution mechanism. The Me groups in the 3,5-positions of the aromatic ring block cyclization reactions which would create a stable *o*-xylylene glycoluril derivative and thereby promote removal of the CH<sub>2</sub>-O-CH<sub>2</sub> residues.

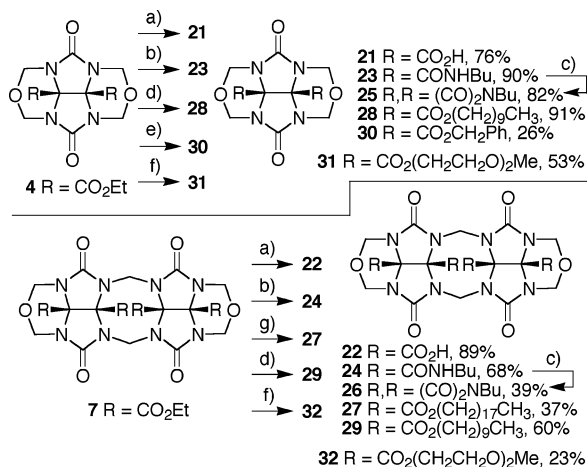
(34) If the formation of macrocycles occurred, we would expect to see a new set of doublets with coupling constants of ~16 Hz at ~5.8 and ~4.5 ppm in the <sup>1</sup>H NMR spectrum. Despite several attempts under a variety of different conditions (acid, concentration, ratios, etc.), we could not obtain any evidence for the formation of macrocyclic CB[*n*] by <sup>1</sup>H NMR analysis.

(35) Drew, H. D. K.; Pearman, F. H. *J. Chem. Soc.* **1937**, 586–592.

(36) Compound **17** is soluble in hot MeSO<sub>3</sub>H but is not soluble in refluxing ClCH<sub>2</sub>CH<sub>2</sub>Cl/PTSA. Therefore, we were unable to perform these macrocyclization reactions with ClCH<sub>2</sub>CH<sub>2</sub>Cl/PTSA.

(37) Although (±)-**20** could be chromatographed on SiO<sub>2</sub> with high recovery, there were significant losses of **19** during SiO<sub>2</sub> chromatography.

(38) Burnett, C. A.; Lagona, J.; Wu, A.; Shaw, J. A.; Coody, D.; Fettinger, J. C.; Day, A. I.; Isaacs, L. *Tetrahedron* **2003**, *59*, 1961–1970.

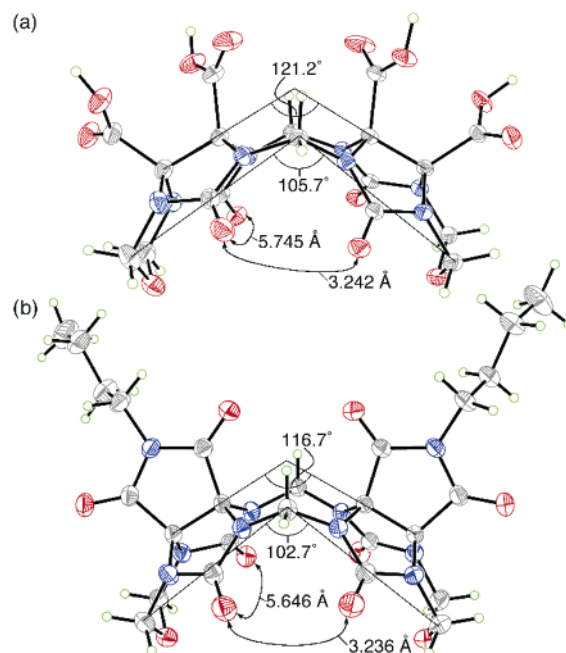
**SCHEME 6. Building Blocks for the Synthesis of CB[n] Analogues<sup>a</sup>**


<sup>a</sup> Conditions: (a) (i) LiOH, CH<sub>3</sub>OH, H<sub>2</sub>O; (ii) HClO<sub>4</sub>, H<sub>2</sub>O; (b) H<sub>2</sub>NBu, neat, 78 °C; (c) ClCH<sub>2</sub>CH<sub>2</sub>Cl, PTSA, reflux; (d) HO(CH<sub>2</sub>)<sub>9</sub>CH<sub>3</sub>, KOCH<sub>3</sub>, 18-crown-6, PhCH<sub>3</sub>, reflux; (e) HOCH<sub>2</sub>Ph, KOCH<sub>3</sub>, 18-crown-6, PhCH<sub>3</sub>, reflux; (f) HO(CH<sub>2</sub>CH<sub>2</sub>O)<sub>2</sub>CH<sub>3</sub>, KOCH<sub>3</sub>, 18-crown-6, PhCH<sub>3</sub>, reflux; (g) HO(CH<sub>2</sub>)<sub>17</sub>CH<sub>3</sub>, KOCH<sub>3</sub>, 18-crown-6, PhCH<sub>3</sub>, reflux.

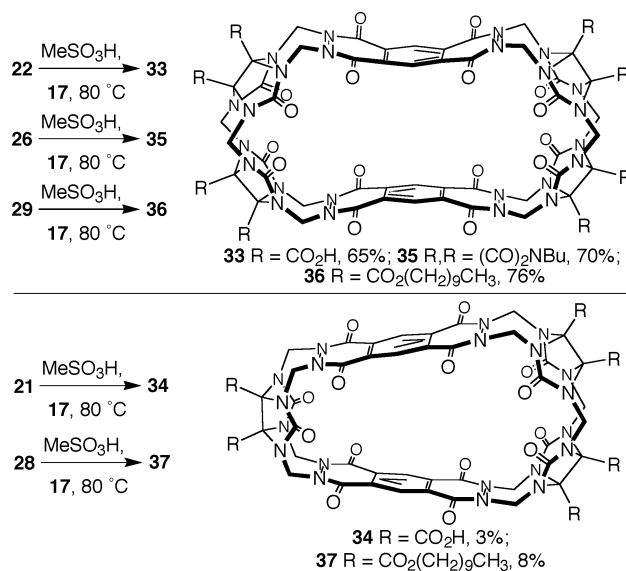
in 37% (Scheme 6). We also performed the transesterification of **4** and **7** with 1-decyl alcohol, which yielded **28** and **29** in 91% and 60% yields, respectively. To assess the generality of these transesterification reactions, we tested several different alcohols and obtained **30**, **31**, and **32** in modest yields (Scheme 6). Apparently, a fine balance of steric and electronic effects influences the efficiency of the 4-fold transesterification. All of these new building blocks possess high solubility in nonpolar solvents such as CDCl<sub>3</sub>, commonly used for our self-assembly studies.

**X-ray Crystal Structures of Building Blocks **22** and **26**.** We obtained crystals of **22** and **26** suitable for X-ray crystal structure determination from aqueous HCl and CH<sub>3</sub>CN, respectively (Figure 3). In this section we discuss some of the structural features of **22** and **26** that influence the preorganization of these building blocks for CB[n] analogue formation. For example, the bond angle through the glycoluril quaternary carbons of **22** (121.2°) and **26** (116.7°) are nearly identical to that observed for CB[6] (118.7°).<sup>40</sup> The bond angle through the methylene bridges of **22** (105.7°) and **26** (102.7°) are somewhat smaller than the corresponding values for CB[5] (110.1°) and CB[6] (116.4°); we attribute this difference to the presence of six-membered cyclic ether rings in **22** and **26**, whereas CB[n] possesses eight-membered rings. The crucial O⋯O distances that define the depth of the macrocycle and the width of its portals for **22** (5.745 and 3.242 Å) and **26** (5.646 and 3.236 Å) are 0.2–0.3 Å shorter than those observed for CB[6] (6.042 and 3.417 Å). In combination, these crystallographic results suggest that building blocks **22** and **26** are preorganized to form CB[5] and/or CB[6] analogues.

**CB[n] Analogues with Enhanced Solubility.** We were pleased to find that when **22** is condensed with **17**,



**FIGURE 3.** ORTEP plots of the X-ray crystal structures of (a) **22** and (b) **26** with 50% probability ellipsoids along with selected distances and angles. Solvent molecules have been omitted for clarity. Color coding: C, gray; H, green; N, blue; O, red.

**SCHEME 7. Synthesis of CB[n] Analogues Soluble in Water and Organic Solvents**


CB[6] analogue **33** is formed in 65% yield and possesses exceptional solubility (~18 mM) in aqueous solutions as determined by gravimetric analysis (Scheme 7). Similarly, the condensation of **21** with **17** gave CB[5] analogue **34**, although in a very disappointing 3% yield after extensive purification. The solubility of **34** in aqueous solutions (~24 mM) is slightly higher than that observed for **33**. These water-soluble CB[5] and CB[6] analogues retain much of the unique binding properties of the CB[n] family with the added properties of long-wave UV–vis and fluorescence activity, which allows for easy detection of the macrocycle under a variety of conditions.<sup>4</sup>

When we submitted **26** to the macrocycle-forming

(39) Brady, P. A.; Bonar-Law, R. P.; Rowan, S. J.; Suckling, C. J.; Sanders, J. K. M. *Chem. Commun.* **1996**, 319–320.

(40) Freeman, W. A.; Mock, W. L.; Shih, N. Y. *J. Am. Chem. Soc.* **1981**, *103*, 7367–7368.

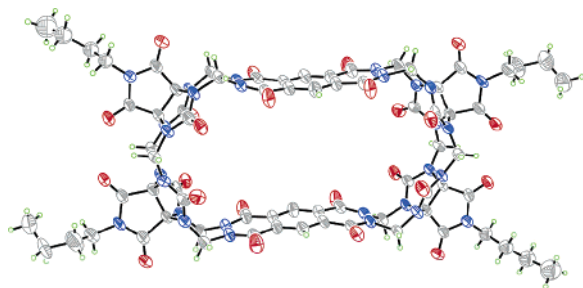


**FIGURE 4.** ORTEP plot of the X-ray crystal structure of **35** with 50% probability ellipsoids. Solvating CH<sub>3</sub>CN molecules within the cavity have been omitted for clarity. Color coding: C, gray; H, green; N, blue; O, red.

reaction conditions we obtained CB[6] analogue **35**, which was poorly soluble in CHCl<sub>3</sub>, in 70% yield. Next, we submitted tetrakis(octadecyl ester) **27** to the reaction conditions and to our surprise discovered that **27** was not soluble in MeSO<sub>3</sub>H. No CB[6] analogue could be obtained with this building block. Apparently, **27** is too lipophilic, which does not allow it to be soluble in the polar acidic solvent (MeSO<sub>3</sub>H). In contrast, the condensation reaction of tetrakis(decyl ester) **29** with **17** proceeded smoothly to give CB[6] analogue **36** in 76% yield (Scheme 7). A similar reaction was performed with **28** and **17**, which delivered CB[5] analogue **37** in 8% yield.<sup>41</sup> Macrocycles **36** and **37** possess excellent solubility (~30 and ~24 mM, respectively) in CHCl<sub>3</sub>; solubility is comparable in CH<sub>2</sub>Cl<sub>2</sub> and THF.

The purification of these new macrocycles with their enhanced characteristics is possible by simple column chromatography, which is important since CB[*n*] cannot be separated using SiO<sub>2</sub> because CB[*n*] are not soluble in solvents appropriate for SiO<sub>2</sub> columns and CB[*n*] are not easily detectable by UV–vis. Therefore, more involved purification techniques have been formulated for the separation and purification of CB[*n*], all of which are laborious. These new CB[*n*] analogues enable studies of their molecular recognition properties in organic solvents and aqueous solution.

The relatively poor solubility of **35** in organic solvents proved beneficial in that crystals suitable for X-ray crystallography could be obtained from CH<sub>3</sub>CN/PhCH<sub>3</sub>. Figure 4 shows the X-ray crystal structure of **35**. Unlike the known cylindrical-shaped CB[*n*], **35** assumes a more elongated-oval shape with cavity dimensions of 5.90 Å × 11.15 Å × 6.92 Å. The O···O distances on the adjacent glycolurils for **35** are 3.424 and 5.930 Å on the same glycoluril, respectively, which are similar to the distances observed for **26** (Figure 3b) and CB[6] (3.417 and 6.042 Å). The bond angles of the adjacent glycolurils through the methylene bridges for **35** (111.8°; CB[6] = 116.4°) and through the quaternary carbons on the glycoluril (120.2°; CB[6] = 118.7°) are comparable. The adjacent glycolurils appear to be slightly pinched in **35** to help compensate for the flat bis(phthalhydrazide) (**17**) incorporated into the macrocycle.

**Mechanistic Studies.** We were surprised that the yields of the CB[6] analogues **18**, **33**, **35**, and **36** were ≥65% given the potential complexity of the intermediates

leading to their formation. This result suggests that the condensation of 2 equiv of bis(cyclic ether) **38** with 1 equiv of bis(phthalhydrazide) **17** is not a random process and the reaction pathway must favor macrocycle formation. Scheme 8 presents a mechanistic hypothesis that details potential intermediates in CB[6] analogue formation. In a common first step, nucleophilic **17** reacts with electrophilic **38** to form **39** by a condensation process. Intermediate **39** can lead to intermediate **40** by reaction with **17** or C- and S-shaped diastereomers **41** and **42** by condensation with **38**. Intermediates **40** and **41** lead to a common intermediate **44**, which is preorganized for macrocyclic formation. Alternatively, both **40** and **42** can lead to S-shaped intermediate **43**, which is prevented from being directly converted to **45** by virtue of the relative stereochemistry of its two methylene bridged glycoluril dimeric subunits. Intermediates **42** and **43** are destined to form oligomers or polymers unless a change from the S-shaped to C-shaped relative orientation of the C-shaped building blocks is feasible. In this section we address key mechanistic questions that provide a rationale for the high yield of CB[6] analogues. In particular, we probe (1) the existence of an equilibrium between **41** and **42** and between **43** and **44** (aqua arrows), (2) the nature of these equilibria (e.g., intra- versus intermolecular; intramolecular **41** ⇌ **42**, intermolecular **41** ⇌ **39** + **17** ⇌ **42**), and (3) the existence of an equilibrium (red arrows) between **44** and **45** (e.g., kinetic versus thermodynamic products).

#### Establishment of an S- to C-Shaped Equilibrium.

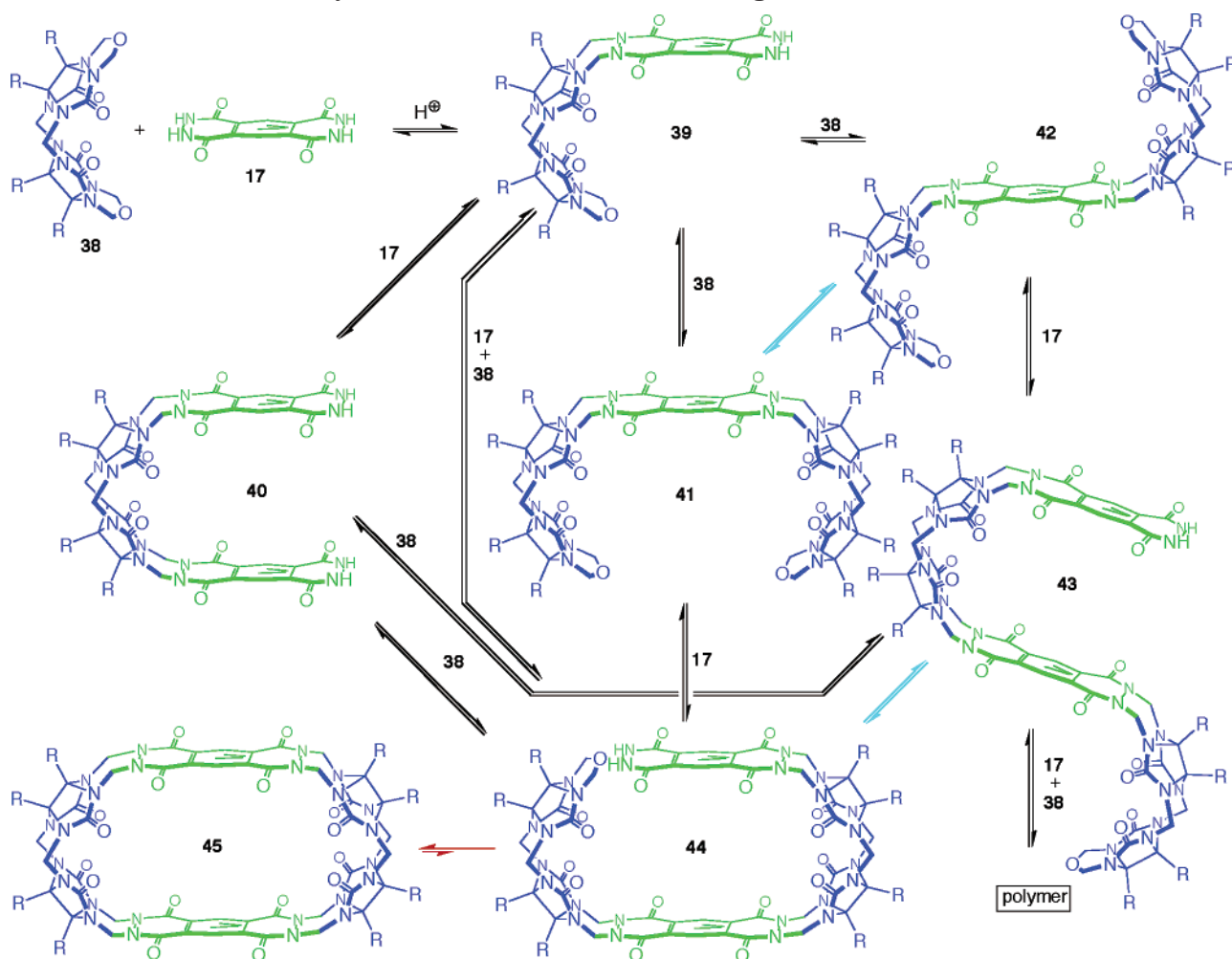
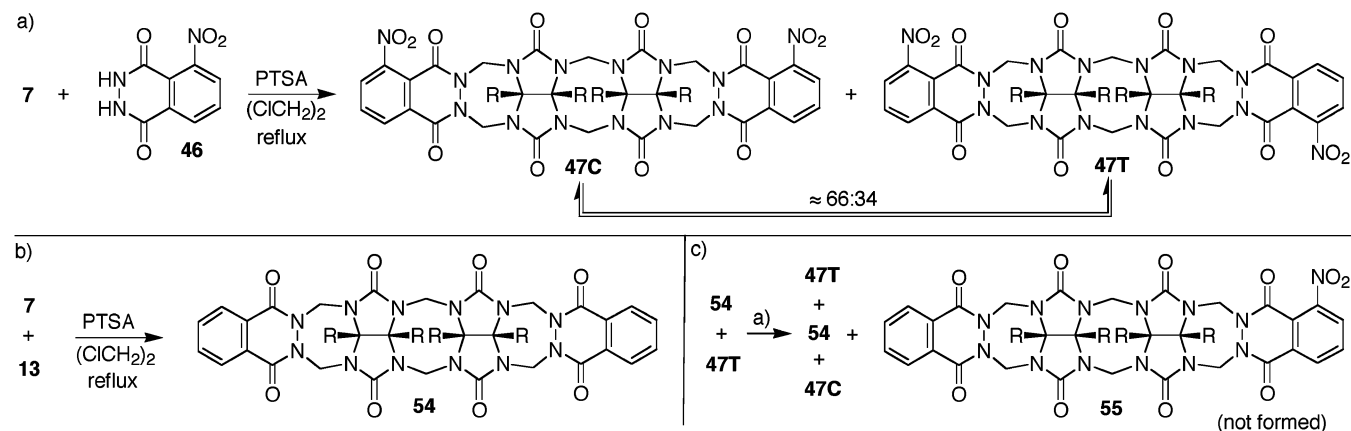
To address the first question, i.e., the potential presence of an equilibrium between **41** and **42** (and **43** and **44**), we adapted a labeling experiment that we had previously used to study the mechanism of CB[*n*] formation.<sup>20,26</sup> For this purpose we reacted **7** and **46** to produce a separable mixture of **47C** and **47T** (Scheme 9a). Compounds **47C** and **47T** were separately resubmitted to the reaction conditions; in both cases we observed a 66:34 ratio of **47C**:**47T**.<sup>42</sup> This experiment establishes an equilibrium between **47C** and **47T** and by analogy suggests an equilibrium between **41** and **42** (**43** and **44**) but does not differentiate between intra- and intermolecular S- to C-shape isomerization.

**Differentiation Between Intramolecular and Intermolecular S- to C-Shaped Isomerization.** Scheme 10 shows proposed mechanistic pathways for the intramolecular isomerization (green arrows) and the intermolecular isomerization (red arrows) for **47C** to **47T**. In brief, compound **47C** initially undergoes protonation and fragmentation to yield *N*-acyliminium ion **48**. Intermediate **48**, under our anhydrous acidic conditions, yields *N*-acylammonium **49** by intramolecular capture by the N-atom. Subsequently, **49** can fragment to either **48** or **50**. Intermediate **50** cyclizes to yield **51**, which loses a proton to give **47T**. Intermolecular isomerization proceeds via intermediates **52** and **53**. To differentiate between intra- versus intermolecular processes in the S- to C-shaped conversion, we resorted to a crossover experiment. For this purpose we prepared **54** by the condensation of **7** and **13** (Scheme 9b). Next we allowed **47T** to isomerize in the presence of **54** (Scheme 9c). If the equilibrium

(41) The crude reaction mixture contains approximately 30% compound **37**.

(42) These isomerization reactions were performed in PTSA/1,2-dichloroethane because **47C** and **47T** are not stable in hot MeSO<sub>3</sub>H.

## SCHEME 8. Possible Pathways in the Formation of CB[6] Analogues

SCHEME 9. (a) Synthesis and Isomerization of **47C** and **47T**. (b) Synthesis of **54**, 71%. (c) Evidence of Mixed Dimer **55** Not Being Formed ( $R = \text{CO}_2\text{Et}$ )<sup>a</sup>

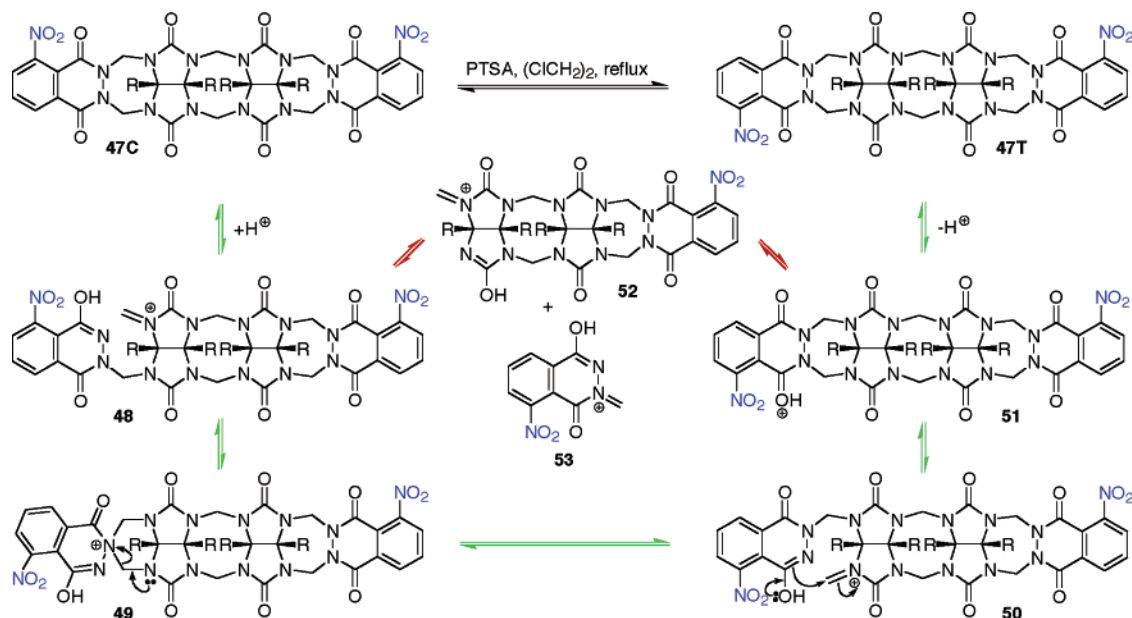
<sup>a</sup> Conditions: (a) PTSA,  $(\text{ClCH}_2)_2$ , reflux.

between **47C** and **47T** is an intramolecular process, then we would only expect to observe homodimeric **54** and **47C/47T** at equilibrium. In contrast, if dissociation of a phthalhydrazide wall is necessary (e.g., intermolecular pathway, red arrows), then we would expect to observe the formation of **54**, **47C**, **47T**, and heterodimer **55**. In the event, we do not observe the formation of **55** under

these conditions.<sup>43</sup> This result establishes an intramolecular isomerization between **47C** and **47T** and suggests

(43) Analysis of the  $^1\text{H}$  NMR spectra as well as TLC provides evidence that only three products result from this reaction: **47C**, **47T**, and **54**. This result establishes that the isomerization of the **47C** and **47T** occurs though an intramolecular mechanism because an intermolecular pathway would result in the formation of mixed dimer **55**.

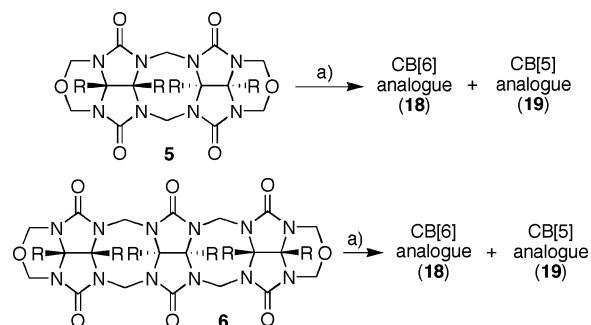


SCHEME 10. Proposed Mechanisms for the Equilibrium between 48C and 48T Dimers (R = CO<sub>2</sub>Et)

similar unimolecular isomerization between **41** and **42** (**43** and **44**; aqua arrows, Scheme 8).

**Stability of CB[n] Analogues.** CB[n] is a very robust family of macrocycles whose stabilities have been tested with several methods.<sup>44</sup> The incorporation of phthalhydrazides into our macrocycles gives rise to useful new properties such as UV-vis, fluorescence, and electrochemical activity. Unfortunately, the incorporation of phthalhydrazides in the macrocycle also leads to the sensitivity to basic conditions (pH > 7). In contrast, the CB[n] analogues are stable under aqueous acidic conditions. To test whether the new CB[n] analogues were kinetic or thermodynamic products, we resubmitted them to the reaction conditions (MeSO<sub>3</sub>H, 80 °C, 24 h). As the solution was heated, a color change was seen from a pale yellow to a dark orange. The <sup>1</sup>H NMR spectrum for each CB[n] analogue showed small peaks in the downfield (H-Ar-phthalhydrazide) region of the <sup>1</sup>H NMR spectrum. Although we could not identify these byproducts, this result establishes that **18**, **19**, and (±)-**20** are not thermodynamically stable under the reaction conditions and therefore represent products formed under kinetic control. This result, in combination with the replacement reaction (**16** + **13** to **14**) detailed in Scheme 4 supports our suggestion that the macrocyclization reaction is reversible (red arrows, Scheme 8).

**S-Shaped Building Blocks Break Apart during Macrocylic Reactions.** Because C-shaped oligomers **7** and **9** form **18** and (±)-**20**, respectively, when reacted with **17**, we were curious to see what would happen if the S-shaped oligomers **5** and **6** were used in place of the C-shaped oligomers. We previously established that the S-shaped **1** and C-shaped **2** are the kinetic products formed, which isomerized under forcing conditions (anhydrous PTSA in CICH<sub>2</sub>CH<sub>2</sub>Cl) to yield **2** by an intramolecular isomerization. The reaction of phthalhydrazides with bis(cyclic ethers) is much faster than the cyclic ether

SCHEME 11. S-Shaped Oligomers **5** and **6** Yield CB[5] and CB[6] Analogues (R = CO<sub>2</sub>Et)<sup>a</sup>

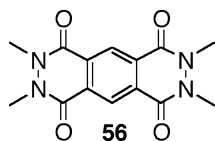
<sup>a</sup> Conditions: (a) **17**, MeSO<sub>3</sub>H, 80 °C.

dimerizing with itself. For example, in the reaction of **12** with **13** (Scheme 4) we do not detect any self-condensation occurring between two molecules of **12**; the formation of compound **14** was exclusively observed.

We attempted these condensation reactions with the S-shaped isomers in order to gain further insight into the mechanism of the formation of CB[n] analogues. In the event, reaction of **5** or **6** with **17** in anhydrous MeSO<sub>3</sub>H yields a mixture of CB[6] analogue (**18**) and CB[5] analogue (**19**) in almost a 1:1 ratio in high overall yield based on the crude <sup>1</sup>H NMR spectrum (Scheme 11), which is similar to the results obtained using **4**, **7**, and **17** (see Scheme 5). This experiment provides indirect evidence that S-shaped building blocks **4** and **7**, which result in the formation of CB[6] and CB[5] analogues (**18** and **19**). In contrast, attempted isomerization experiments using only **5** or **6** leads to further oligomerization rather than isomerization, which was evident by broad peaks in the <sup>1</sup>H NMR spectrum of the crude reaction mixture. Apparently, the presence of (bis)phthalhydrazide **17** in the reaction mixture changes the kinetics and thermodynamics of the reaction by providing an in situ self-protection

(44) Buschmann, H. J.; Jansen, K.; Meschke, C.; Schollmeyer, E. *J. Solution Chem.* **1998**, *27*, 135–140.

## CHART 2. Template Molecule



of compounds **5** or **6**, preventing further oligomerization resulting in the formation of macrocyclic products **18** and **19**.

**Template Effects.** To address whether template effects are important in the formation of the CB[6] analogues, we performed two experiments. First, we performed the macrocyclization in the presence of 1 equiv of **56** (Chart 2) as a potential template that is unreactive under the reaction conditions. Even though **56** does not bind to **18** in MeSO<sub>3</sub>H, it may still partake in favorable  $\pi$ - $\pi$  interactions with intermediates **40** and **44** (see Scheme 8) that lead to **18** and thereby template its formation. When we conducted the reaction between **7** (2 equiv) and **17** (2 equiv) in the presence of potential template **56** (1 equiv), we isolated **18** in 59% yield, which is slightly lower than that observed in its absence.<sup>45</sup>

As a second test for potential templation effects, we performed the macrocyclization at a series of different concentrations (147, 44, and 22 mM) to discern if **40** (or other intermediates) act as templates for the formation of the CB[6] analogues. In these experiments, the isolated yields of CB[6] analogue **18** were 78%, 74%, and 70%, respectively. There is a slight decrease in the isolated yield as the reaction concentration is decreased, but it is minimal. The combined inference of both sets of experiments is that templation effects are not important in the formation of CB[6] analogues.

## Conclusion

The synthesis of CB[*n*] analogues with outstanding solubility characteristics in both water and organic solution has been presented with the focus on functionalization and mechanistic studies. C-shaped building blocks (e.g., **7** and **9**) are preorganized for macrocycle formation, whereas their S-shaped diastereomers (e.g., **5** and **6**) undergo fragmentation reactions concomitant with macrocyclization. The mechanistic studies have established the intramolecular S- to C-shaped isomerization as a key step in the synthesis of the CB[6] analogues. In contrast to the unfunctionalized cucurbiturils, the macrocyclization that delivers the CB[*n*] analogues is under kinetic rather than thermodynamic control and is not subject to the effects of templation. The properties of the new CB[*n*] analogues are enhanced by the incorporation of the bis(phthalhydrazide) walls, which endow them with UV-vis, fluorescence, and electrochemical activity.

The insights derived from our study of the mechanism of formation of the CB[6] analogues suggest methods for the expansion of the synthetic method to the production

of different CB[*n*] analogues of greater stability and functionality. In addition, although the building block approach has only been exploited using bis(phthalhydrazide) **17**, we envision that longer and nonplanar bis(phthalhydrazides) as well as other nucleophilic glycoluril surrogates should perform equally well in these macrocyclization reactions. The ability to increase the size of the cavity would allow for different binding properties (e.g., the formation of termolecular and higher molecularity complexes) as well as different optical properties depending on the glycoluril surrogate incorporated into the macrocycle. Currently, these new CB[6] analogues, both the aqueous and organic soluble macrocycles, are being studied to evaluate their potential for application as components of molecular machines, in self-sorting systems, and as fluorescent sensors for chemically and biologically important amines.

## Experimental Section

**Compound 11.** Compound **7** (0.200 g, 0.293 mmol) and 3,5-dimethylphenol (0.895 g, 7.325 mmol) were dissolved in TFA (10 mL). The reaction mixture was stirred and heated at reflux for 24 h. The reaction mixture was concentrated and dried under high vacuum. The residue was washed with Et<sub>2</sub>O (3 × 10 mL), centrifuged, and dried under high vacuum. The resulting powder was recrystallized from EtOH (30 mL) to give **11** as a white solid which was centrifuged and dried under high vacuum (0.110 g, 0.185 mmol, 63%). Mp > 350 °C. TLC (CHCl<sub>3</sub>/CH<sub>3</sub>OH, 5:1) *R<sub>f</sub>* 0.11. IR (KBr, cm<sup>-1</sup>): 3456s, 3344s, 2983w, 2936w, 1750s, 1719s, 1630w, 1448s, 1370m, 1269s, 1238s, 1160w, 1036m, 1005m. <sup>1</sup>H NMR (400 MHz, DMSO-*d*<sub>6</sub>): 8.84 (s, 4H), 5.79 (d, *J* = 15.8, 2H), 4.22 (d, *J* = 15.8, 2H), 4.16 (q, *J* = 7.2, 4H), 4.11 (q, *J* = 7.2, 4H), 1.19 (t, *J* = 7.2, 6H), 1.17 (t, *J* = 7.2, 6H). <sup>13</sup>C NMR (100 MHz, DMSO-*d*<sub>6</sub>): 166.9, 165.8, 156.7, 82.1, 74.7, 63.8, 63.3, 47.0, 14.1, 14.0. MS (FAB, Magic Bullet): *m/z* 597 (100, [M + H]<sup>+</sup>). HR-MS (FAB, Magic Bullet): *m/z* 597.1896 ([M + H]<sup>+</sup>, C<sub>22</sub>H<sub>29</sub>N<sub>8</sub>O<sub>12</sub>, calcd 597.1905).

**Compound 14. Method 1.** A mixture of PTSA (0.388 g, 2.04 mmol) and ClCH<sub>2</sub>CH<sub>2</sub>Cl (15 mL) was heated under N<sub>2</sub> at reflux for 30 min under an addition funnel filled with molecular sieves (4 Å). Phthalhydrazide (**13**) (0.099 g, 0.612 mmol) and compound **12** (0.200 g, 0.408 mmol) were added and reflux was continued for 3 h. The reaction mixture was diluted with CHCl<sub>3</sub> (100 mL), washed with saturated Na<sub>2</sub>CO<sub>3</sub> and then brine, dried over anhydrous MgSO<sub>4</sub>, and concentrated. Flash chromatography (SiO<sub>2</sub>, CHCl<sub>3</sub>/CH<sub>3</sub>CN 5:1) gave **14** (0.178 g, 0.280 mmol, 69%). **Method 2.** A mixture of PTSA (0.081 g, 0.428 mmol) and ClCH<sub>2</sub>CH<sub>2</sub>Cl (5 mL) was heated under N<sub>2</sub> at reflux for 30 min under an addition funnel filled with molecular sieves (4 Å). Compound **16** (0.050 g, 0.086 mmol) and paraformaldehyde (0.013 g, 0.428 mmol) were added and reflux was continued for 24 h. Compound **13** (0.014 g, 0.428 mmol) was added and reflux was continued for 4 h. The reaction mixture was diluted with EtOAc (100 mL), washed with saturated Na<sub>2</sub>CO<sub>3</sub> and then brine, dried over anhydrous MgSO<sub>4</sub>, and concentrated. Flash chromatography (SiO<sub>2</sub>, CHCl<sub>3</sub>/CH<sub>3</sub>CN 5:1) gave **14** (0.044 g, 0.069 mmol, 81%). Mp > 300 °C (dec). TLC (CHCl<sub>3</sub>/CH<sub>3</sub>CN, 5:1) *R<sub>f</sub>* 0.15. IR (KBr, cm<sup>-1</sup>): 2983w, 2940w, 2851w, 1758s, 1736s, 1643s, 1608m, 1522m, 1468s, 1449s, 1429s, 1340m, 1305s, 1262s, 1150m, 1134m, 1103s, 1049m, 1025m. <sup>1</sup>H NMR (400 MHz, CDCl<sub>3</sub>): 8.24 (br. s, 2H), 7.73 (br. s, 2H), 7.13 (d, *J* = 15.7, 2H), 6.74 (s, 2H), 4.70 (d, *J* = 16.0, 2H), 4.68 (d, *J* = 15.7, 2H), 4.45 (d, *J* = 16.0, 2H), 4.35–4.25 (m, 4H), 3.79 (s, 6H), 1.40–1.30 (m, 6H). <sup>13</sup>C NMR (100 MHz, CDCl<sub>3</sub>): 165.2, 165.0, 156.5, 154.3, 147.9, 133.6, 128.4, 128.2, 113.3, 80.0, 64.0, 63.6, 55.9, 51.2, 45.3, 14.0, 13.9 (only 17 of the 19 expected resonances were observed). MS (FAB, Magic Bullet): *m/z* 635 (100, [M + H]<sup>+</sup>). HR-MS (FAB,

(45) The experiments detailed here do not provide evidence of template effects operating in the formation of CB[6] analogues. An alternative rationale for the high yields observed in this four-component macrocyclization lies in the preorganized shape of the building blocks. For example, the structural features of **7** and **17** (e.g., bond and torsional angles) are such that mixtures of these building blocks have few choices other than macrocyclization.

Magic Bullet):  $m/z$  635.2112 ( $[M + H]^+$ ,  $C_{30}H_{31}N_6O_{10}$ , calcd 635.2102). Anal. Calcd for  $C_{30}H_{30}N_6O_{10}$  (634.59): C 56.78, H 4.76. Found: C 56.75, H 4.81.

**Compound 16.** Compound **12** (0.300 g, 0.612 mmol) and 3,6-dihydroxypyridazine (**15**) (0.102 g, 0.912 mmol) were dissolved in TFA (6 mL). The mixture was stirred at reflux for 48 h and then was concentrated and dried under high vacuum. The crude material was recrystallized from boiling EtOH (100 mL) to give **16** as a light-pink crystalline solid (0.198 g, 0.339 mmol, 55%). Mp 281–283 °C. TLC ( $CHCl_3/CH_3OH$ , 10:1)  $R_f$  0.35. IR (KBr,  $cm^{-1}$ ): 3080w, 3002w, 2979w, 2955w, 2936w, 2920w, 1755s, 1728s, 1662s, 1522m, 1464s, 1445s, 1425s, 1336m, 1301m, 1258s, 1223m, 1107m.  $^1H$  NMR (400 MHz,  $CDCl_3$ ): 6.93 (d,  $J = 15.6$ , 2H), 6.78 (s, 2H), 6.75 (s, 2H), 4.71 (d,  $J = 16.0$ , 2H), 4.59 (d,  $J = 15.6$ , 2H), 4.45 (d,  $J = 16.0$ , 2H), 4.35–4.25 (m, 4H), 3.84 (s, 6H), 1.35–1.30 (m, 6H).  $^{13}C$  NMR (100 MHz,  $CDCl_3$ ): 165.0, 164.9, 155.3, 154.2, 147.9, 134.8, 128.2, 113.3, 80.1, 64.1, 63.6, 56.0, 50.6, 45.3, 14.0, 13.9 (only 16 of the 17 expected resonances were observed). MS (FAB, Magic Bullet):  $m/z$  585 (73,  $[M + H]^+$ ), 206 (100,  $[C_{11}H_{12}NO_3]^+$ ). HR-MS (FAB, Magic Bullet):  $m/z$  585.1957 ( $[M + H]^+$ ,  $C_{26}H_{29}N_6O_{10}$ , calcd 585.1945). Anal. Calcd for  $C_{26}H_{28}N_6O_{10}$  (584.53): C 53.42, H 4.83. Found: C 53.19, H 4.92.

**Compound 27.** A solution of **7** (0.100 g, 0.147 mmol) and 1-octadecanol (0.397 g, 1.47 mmol) in toluene (30 mL) was heated under  $N_2$  at reflux for 30 min under an addition funnel filled with molecular sieves (4 Å). A premade solution of 18-crown-6 (0.020 g, 0.0735 mmol) and  $KOCH_3$  (0.005 g, 0.0735 mmol) in toluene/ $CH_3OH$  (0.6 mL, 5:1) was added to the reaction mixture and reflux was continued for 20 h. The reaction mixture was concentrated and dried under high vacuum. Flash chromatography ( $SiO_2$ ,  $CHCl_3/CH_3CN$  20:1) gave **27** as a white solid (0.090 g, 0.057 mmol, 37%). Mp 161–163 °C. TLC ( $CHCl_3/CH_3CN$ , 20:1)  $R_f$  0.28. IR (KBr,  $cm^{-1}$ ): 2959m, 2917s, 2851s, 1767s, 1468m, 1437m, 1421m, 1297m, 1251s, 1091m, 1072m, 1017m, 1010m.  $^1H$  NMR (400 MHz,  $CDCl_3$ ): 5.99 (d,  $J = 16.0$ , 2H), 5.53 (d,  $J = 11.0$ , 4H), 4.86 (d,  $J = 16.0$ , 2H), 4.73 (d,  $J = 11.0$ , 4H), 4.20–4.10 (m, 8H), 1.65–1.55 (m, 8H), 1.30–1.20 (m, 120H), 0.86 (t,  $J = 6.8$ , 12H).  $^{13}C$  NMR (100 MHz,  $CDCl_3$ ): 165.4, 164.9, 155.5, 79.5, 77.1, 74.5, 73.2, 68.6, 68.2, 63.5, 48.7, 33.2, 32.4, 30.1, 30.1, 30.0, 29.9, 29.9, 29.8, 29.6, 29.5, 28.8, 28.5, 26.2, 26.1, 26.1, 23.1, 14.6 (only 28 of the 43 expected resonances were observed). MS (FAB, Magic Bullet/PEG):  $m/z$  1579 (100,  $[M + H]^+$ ).

**Compound 28.** A solution of **4** (0.100 g, 0.273 mmol) and 1-decanol (0.52 mL, 2.73 mmol) in toluene (30 mL) was heated under  $N_2$  at reflux for 30 min under an addition funnel filled with molecular sieves (4 Å). A premade solution of 18-crown-6 (0.007 g, 0.027 mmol) and  $KOCH_3$  (0.002 g, 0.027 mmol) in toluene/ $CH_3OH$  (0.6 mL, 5:1) was added to the reaction mixture and reflux was continued for 20 h. The reaction mixture was concentrated and dried under high vacuum. Flash chromatography ( $SiO_2$ ,  $CHCl_3/CH_3CN$  50:1) gave **28** as a white solid (0.146 g, 0.245 mmol, 91%). Mp 54–55 °C. TLC ( $CHCl_3/CH_3CN$ , 25:1)  $R_f$  0.31. IR (KBr,  $cm^{-1}$ ): 2959m, 2924s, 2851m, 1775s, 1748s, 1472m, 1410m, 1383s, 1297s, 1235s, 1169m, 1107m, 1068m, 1041m, 1029m, 1002m.  $^1H$  NMR (400 MHz,  $CDCl_3$ ): 5.53 (d,  $J = 11.2$ , 4H), 4.81 (d,  $J = 11.2$ , 4H), 4.20 (t,  $J = 6.9$ , 4H), 1.65–1.60 (m, 4H), 1.30–1.20 (m, 28H), 0.86 (t,  $J = 6.8$ , 6H).  $^{13}C$  NMR (100 MHz,  $CDCl_3$ ): 164.8, 156.9, 74.5, 72.5, 67.9, 31.9, 29.6, 29.5, 29.4, 29.2, 28.3, 25.8, 22.8, 14.2. MS (FAB, Magic Bullet/LiCl):  $m/z$  602 (100,  $[M + Li]^+$ ). HR-MS (FAB, Magic Bullet/LiCl):  $m/z$  601.3793 ( $[M + Li]^+$ ,  $C_{30}H_{50}N_4O_8Li$ , calcd 601.3789).

**Compound 29.** A solution of **7** (0.100 g, 0.147 mmol) and 1-decanol (0.56 mL, 2.94 mmol) in toluene (80 mL) was heated under  $N_2$  at reflux for 30 min under an addition funnel filled with molecular sieves (4 Å). A premade solution of 18-crown-6 (0.020 g, 0.074 mmol) and  $KOCH_3$  (0.005 g, 0.074 mmol) in toluene/ $CH_3OH$  (0.6 mL, 5:1) was added to the reaction mixture and reflux was continued for 20 h. The reaction mixture was concentrated and dried under high vacuum. Flash

chromatography ( $SiO_2$ ,  $CHCl_3/CH_3CN$  40:1) gave **29** as a white solid (0.100 g, 0.089 mmol, 60%). Mp 169–171 °C. TLC ( $CHCl_3/CH_3CN$ , 25:1)  $R_f$  0.15. IR (KBr,  $cm^{-1}$ ): 2955m, 2928s, 2854m, 1763s, 1468m, 1429m, 1414m, 1297m, 1270m, 1251s, 1087m, 1068m, 1017m, 1006m.  $^1H$  NMR (400 MHz,  $CDCl_3$ ): 5.99 (d,  $J = 16.0$ , 2H), 5.52 (d,  $J = 10.9$ , 4H), 4.85 (d,  $J = 16.0$ , 2H), 4.73 (d,  $J = 10.9$ , 4H), 4.20–4.10 (m, 8H), 1.65–1.60 (m, 8H), 1.30–1.20 (m, 56H), 0.86 (t,  $J = 6.6$ , 12H).  $^{13}C$  NMR (100 MHz,  $CDCl_3$ ): 165.0, 164.5, 155.1, 79.0, 74.0, 72.7, 68.1, 67.8, 48.2, 31.8, 29.5, 29.5, 29.4, 29.3, 29.2, 29.1, 29.1, 28.2, 28.1, 25.7, 25.7, 22.6, 14.1 (only 23 of the 27 expected resonances were observed). MS (FAB, Magic Bullet/CsI):  $m/z$  1261 (100,  $[M + Cs]^+$ ). HR-MS (FAB, Magic Bullet/CsI):  $m/z$  1261.6061 ( $[M + Cs]^+$ ,  $C_{58}H_{96}N_8O_{14}Cs$ , calcd 1261.6100).

**Compound 34.** A mixture of **17** (0.214 g, 0.870 mmol) and anhydrous  $MeSO_3H$  (5 mL) was stirred at 80 °C until homogeneous. Compound **21** (0.540 g, 0.870 mmol) was added in one portion and the flask was sealed and heated at 80 °C for 3 h. The reaction mixture was cooled to room temperature and then poured into acetone (50 mL). The solid was collected by filtration, washed with additional acetone (50 mL), and dried under high vacuum overnight to yield crude material as a yellow solid (0.744 g). The crude material (0.300 g) was purified by ion-exchange chromatography (Cellulose-DEAE) with sodium acetate buffer (pH = 5.7, 100 mM). After loading the material on the column, increasing the NaCl gradient from 5% to 15% gave **34** contaminated with salts (NaOAc and NaCl). These salts were removed using size exclusion chromatography (Sephadex G-25) to yield **34** as a pale yellow solid (0.015 g, 0.012 mmol, 3%). Mp > 350 °C (dec). IR (KBr,  $cm^{-1}$ ): 2963w, 2924w, 2847w, 1732m, 1717m, 1654s, 1468m, 1386m, 1297m, 1239m, 1153w, 1103m.  $^1H$  NMR (400 MHz,  $D_2O$ ): 8.72 (s, 4H), 6.90 (d,  $J = 16.1$ , 4H), 6.81 (d,  $J = 15.9$ , 4H), 5.54 (d,  $J = 16.1$ , 2H), 5.00 (d,  $J = 16.1$ , 2H), 4.99 (d,  $J = 16.1$ , 4H), 4.87 (d,  $J = 15.9$ , 4H).  $^{13}C$  NMR (100 MHz,  $D_2O$ ): 168.8, 168.5, 156.7, 156.6, 156.1, 156.0, 131.8, 131.1, 128.6, 81.7, 79.6, 51.8, 50.5, 48.7 (only 14 of the 16 expected resonances were observed). MS (ESI):  $m/z$  1325 (100,  $[M + Na]^+$ ). HR-MS (ESI):  $m/z$  1325.1621 ( $[M + Na]^+$ ,  $C_{48}H_{30}N_{20}O_{26}Na$ , calcd 1325.1538).

**Compound 36.** A mixture of **17** (0.022 g, 0.147 mmol) and anhydrous  $MeSO_3H$  (2 mL) was stirred at 80 °C until homogeneous. Compound **29** (0.100 g, 0.089 mmol) was added in one portion and the flask was sealed and heated at 80 °C for 3 h. The reaction mixture was cooled to room temperature and then poured into water (10 mL). The solid was collected by centrifugation and the resulting pellet was resuspended in water (10 mL) and centrifuged again, and then dried under high vacuum overnight to yield **36** as a pale yellow solid (0.090 g, 0.034 mmol, 76%). Mp > 350 °C (dec). TLC ( $CHCl_3/CH_3OH$ , 10:1)  $R_f$  0.10. IR (KBr,  $cm^{-1}$ ): 2959m, 2924s, 2854m, 1755s, 1654s, 1645s, 1635s, 1261s, 1232m, 1165w, 1094m, 1053m, 1025m.  $^1H$  NMR (400 MHz,  $DMSO-d_6$ ): 8.66 (s, 4H), 6.80 (d,  $J = 15.4$ , 8H), 5.88 (d,  $J = 15.6$ , 4H), 5.10 (d,  $J = 15.4$ , 8H), 4.70 (d,  $J = 15.6$ , 4H), 4.20–4.10 (m, 16H), 1.65–1.50 (m, 16H), 1.22 (s, 112H), 0.85–0.80 (m, 24H).  $^{13}C$  NMR (100 MHz,  $CDCl_3$ ): 164.9, 164.7, 155.3, 153.7, 132.0, 129.6, 116.9, 78.5, 78.1, 69.2, 68.9, 53.2, 48.8, 32.3, 30.0, 29.99, 29.96, 29.88, 29.84, 29.7, 29.6, 28.6, 28.5, 26.1, 26.0, 23.1, 14.5 (only 27 of the 30 expected resonances were observed). MS (ESI):  $m/z$  1362 (100,  $[M + 2Na]^{2+}$ ).

**Compound 37.** A mixture of **17** (0.036 g, 0.147 mmol) and anhydrous  $MeSO_3H$  (1 mL) was stirred at 80 °C until homogeneous. Compound **28** (0.130 g, 0.220 mmol) was added in one portion and the flask was sealed and heated at 80 °C for 3 h. The reaction mixture was cooled to room temperature and then poured into water (10 mL). The solid was collected by centrifugation and the resulting pellet was resuspended in water (10 mL) and centrifuged. The solid was dried under high vacuum overnight. Flash chromatography ( $SiO_2$ ,  $CHCl_3/MeOH$  10:1) gave **37** as a pale yellow solid (0.025 g, 0.0115 mmol, 8%). Mp > 350 °C (dec). TLC ( $CHCl_3/CH_3CN$ , 10:1)  $R_f$  0.18. IR (KBr,  $cm^{-1}$ ): 2955m, 2924s, 2854m, 1759s, 1666m, 1464m,

1421m, 1383w, 1262s, 1231s, 1153m, 1099w, 1021w.  $^1\text{H}$  NMR (400 MHz,  $\text{CDCl}_3$ ): 8.92 (s, 4H), 7.18 (d,  $J = 16.0$ , 4H), 7.14 (d,  $J = 16.0$ , 4H), 6.05 (d,  $J = 16.2$ , 2H), 4.79 (d,  $J = 16.0$ , 4H), 4.74 (d,  $J = 16.0$ , 4H), 4.68 (d,  $J = 16.2$ , 2H), 4.30–4.10 (m, 12H), 1.75–1.55 (m, 12H), 1.30–1.20 (m, 84H), 0.90–0.80 (m, 18H).  $^{13}\text{C}$  NMR (125 MHz,  $\text{CDCl}_3$ ): 165.3, 165.0, 164.9, 155.2, 154.9, 153.6, 132.3, 132.1, 130.8, 78.9, 69.4, 69.2, 51.6, 51.2, 49.1, 32.6, 30.3, 30.2, 30.1, 29.9, 29.8, 29.0, 28.9, 28.8, 26.4, 26.3, 23.4, 14.9 (only 28 of the 44 expected resonances were observed). MS (ESI):  $m/z$  2144 (100,  $[\text{M} + \text{H}]^+$ ). HR-MS (ESI):  $m/z$  2144.1139 ( $[\text{M} + \text{H}]^+$ ,  $\text{C}_{108}\text{H}_{51}\text{N}_{20}\text{O}_{26}$ , calcd 2144.1108).

**Compound 47T and 47C.** A mixture of PTSA (0.279 g, 1.47 mmol) and  $\text{ClCH}_2\text{CH}_2\text{Cl}$  (20 mL) was heated under  $\text{N}_2$  at reflux for 30 min under an addition funnel filled with molecular sieves (4 Å). Compound **46** (0.152 g, 0.735 mmol) was added and reflux was continued for 5 min. Compound **7** (0.200 g, 0.294 mmol) was added and reflux was continued for 22 h. The reaction mixture was concentrated and dried under high vacuum. The reaction mixture was diluted with  $\text{CH}_2\text{Cl}_2$  (350 mL), washed with saturated  $\text{Na}_2\text{CO}_3$  and then brine, dried over anhydrous  $\text{MgSO}_4$ , concentrated, and dried under high vacuum. Flash chromatography ( $\text{SiO}_2$ ,  $\text{CHCl}_3/\text{CH}_3\text{CN}$  5:1, then  $\text{CHCl}_3/\text{CH}_3\text{CN}$  4:1) gave **47T** (0.115 g, 0.109 mmol, 37%), **47C** (0.105 g, 0.099 mmol, 34%), and a mixture of **47T/47C** (0.065 g, 0.061 mmol, 21%). **47T**: Mp > 350 °C (dec). TLC ( $\text{CHCl}_3/\text{CH}_3\text{CN}$ , 1:1)  $R_f$  0.14. IR (KBr,  $\text{cm}^{-1}$ ): 3039w, 2983w, 2924w, 2851w, 1751s, 1635s, 1608m, 1546m, 1460m, 1441m, 1417m, 1383w, 1371w, 1309w, 1274s, 1258m, 1153m, 1087w, 1068w, 1052w, 1025m.  $^1\text{H}$  NMR (400 MHz,  $\text{CD}_3\text{CN}$ ): 8.30–8.25 (m, 2H), 7.95–7.85 (m, 2H), 7.80–7.75 (m, 2H), 6.96 (d,  $J = 16.0$ , 2H), 6.87 (d,  $J = 16.0$ , 2H), 5.87 (d,  $J = 16.2$ , 2H), 4.81 (d,  $J = 15.9$ , 2H), 4.79 (d,  $J = 15.9$ , 2H), 4.62 (d,  $J = 16.2$ , 2H), 4.26 (q,  $J = 7.13$ , 8H), 1.30–1.20 (m, 12H).  $^{13}\text{C}$  NMR (100 MHz,  $\text{CD}_3\text{CN}$ ): 165.7, 165.2, 154.8, 154.2, 153.9, 152.7, 149.5, 135.7, 130.8, 130.7, 128.0, 119.6, 79.2, 77.4, 65.6, 65.4, 50.8, 50.6, 48.6, 13.8, 13.7. MS (FAB, Magic Bullet):  $m/z$  1081 (100,  $[\text{M} + \text{Na}]^+$ ). HR-MS (FAB, Magic Bullet):  $m/z$  1191.1415 ( $[\text{M} + \text{Cs}]^+$ ,  $\text{C}_{42}\text{H}_{38}\text{N}_{14}\text{O}_{20}\text{-Cs}$ , calcd 1191.1441). **47C**: Mp > 350 °C (dec). TLC ( $\text{CHCl}_3/\text{CH}_3\text{CN}$ , 1:1)  $R_f$  0.10. IR (KBr,  $\text{cm}^{-1}$ ): 3088w, 3025w, 2983w, 2936w, 1755s, 1647s, 1604w, 1546s, 1464s, 1445s, 1421m, 1375m, 1348w, 1309m, 1270s, 1173w, 1153m, 1095w, 1068w, 1021m.  $^1\text{H}$  NMR (400 MHz,  $\text{CD}_3\text{CN}$ ): 8.25–8.20 (m, 2H), 7.95–7.90 (m, 2H), 7.85–7.80 (m, 2H), 6.92 (d,  $J = 15.9$ , 2H), 6.89 (d,  $J = 16.0$ , 2H), 5.87 (d,  $J = 16.2$ , 1H), 5.85 (d,  $J = 16.2$ , 1H), 4.81 (d,  $J = 15.9$ , 2H), 4.80 (d,  $J = 16.0$ , 2H), 4.67 (d,  $J = 16.3$ , 1H), 4.56 (d,  $J = 16.3$ , 1H), 4.30–4.20 (m, 8H), 1.30–1.20 (m, 12H).  $^{13}\text{C}$  NMR (100 MHz,  $\text{CD}_3\text{CN}$ ): 165.7, 165.2, 154.8, 154.2, 154.1, 152.7, 149.5, 135.9, 131.0, 130.7, 128.0, 119.5, 79.2, 77.4, 65.6, 65.4, 50.8, 50.7, 48.6, 48.5, 13.8, 13.7. MS (FAB, Magic Bullet):  $m/z$  1081 (100,  $[\text{M} + \text{Na}]^+$ ). HR-MS (FAB, Magic Bullet):  $m/z$  1191.1447 ( $[\text{M} + \text{Cs}]^+$ ,  $\text{C}_{42}\text{H}_{38}\text{N}_{14}\text{O}_{20}\text{-Cs}$ , calcd 1191.1441).

**Compound 54.** A mixture of PTSA (0.069 g, 0.365 mmol) and  $\text{ClCH}_2\text{CH}_2\text{Cl}$  (5 mL) was heated under  $\text{N}_2$  at reflux for 30 min under an addition funnel filled with molecular sieves (4 Å). Phthalhydrazide (**13**) (0.026 g, 0.161 mmol) and compound **7** (0.050 g, 0.073 mmol) were added and after 4 h at reflux a

precipitate formed. The reaction mixture was concentrated and dried under high vacuum. The residue was washed with water (3 × 10 mL) and centrifuged to yield **54** as a white solid (50.0 mg, 0.0516 mmol, 71%). Mp 310–312 °C (dec). TLC ( $\text{CHCl}_3/\text{CH}_3\text{CN}$ , 10:1)  $R_f$  0.20. IR (KBr,  $\text{cm}^{-1}$ ): 2990w, 2971w, 1755s, 1635m, 1464m, 1445m, 1398w, 1371w, 1274s, 1161w, 1138m, 1091w, 1021m.  $^1\text{H}$  NMR (400 MHz,  $\text{DMSO}-d_6$ ): 7.80 (br. s, 4H), 7.60 (br. s, 4H), 6.70 (d,  $J = 15.6$ , 4H), 5.88 (d,  $J = 16.2$ , 2H), 5.03 (d,  $J = 15.6$ , 4H), 4.64 (d,  $J = 16.2$ , 2H), 4.30–4.20 (m, 8H), 1.26 (t,  $J = 7.2$ , 6H), 1.23 (t,  $J = 7.2$ , 6H).  $^{13}\text{C}$  NMR (100 MHz,  $\text{DMSO}-d_6$ ): 164.8, 164.2, 155.1, 153.5, 137.4, 78.5, 77.6, 65.3, 64.9, 50.4, 48.2, 14.0, 13.9 (only 13 of the 15 expected resonances were observed). MS (FAB, Magic Bullet):  $m/z$  991 (100,  $[\text{M} + \text{Na}]^+$ ), 969 (45,  $[\text{M} + \text{H}]^+$ ). HR-MS (FAB, Magic Bullet):  $m/z$  969.2802 ( $[\text{M} + \text{H}]^+$ ,  $\text{C}_{42}\text{H}_{41}\text{N}_{12}\text{O}_{16}$ , calcd 969.2763).

**Isomerization Experiments. Isomerization of 47T.** A mixture of PTSA (0.010 g, 0.050 mmol) and  $\text{ClCH}_2\text{CH}_2\text{Cl}$  (5 mL) was heated under  $\text{N}_2$  at reflux for 30 min under an addition funnel filled with molecular sieves (4 Å). Compound **47T** (0.010 g, 0.010 mmol) was added and reflux was continued for 5 d. The reaction mixture was diluted with  $\text{CHCl}_3$  (20 mL), washed with water, dried over  $\text{MgSO}_4$ , and dried under high vacuum. The crude  $^1\text{H}$  NMR was taken in  $\text{DMSO}-d_6$  and the relative ratios of the aromatic peaks at 8.36 and 8.27 ppm were measured by integration to give **47T/47C** in a 36:64 ratio. **Isomerization of 47C.** A mixture of PTSA (0.010 g, 0.050 mmol) and  $\text{ClCH}_2\text{CH}_2\text{Cl}$  (5 mL) was heated under  $\text{N}_2$  at reflux for 30 min under an addition funnel filled with molecular sieves (4 Å). Compound **47C** (0.010 g, 0.010 mmol) was added and reflux was continued for 5 d. The reaction mixture was diluted with  $\text{CHCl}_3$  (20 mL), washed with water, dried over  $\text{MgSO}_4$ , and dried under high vacuum. The crude  $^1\text{H}$  NMR was taken in  $\text{DMSO}-d_6$  and the relative ratios of the aromatic peaks at 8.36 and 8.27 ppm were measured by integration to give **47T/47C** in a 32:68 ratio. **Crossover experiment for 54 and 47T.** A mixture of PTSA (0.010 g, 0.050 mmol) and  $\text{ClCH}_2\text{-CH}_2\text{Cl}$  (5 mL) was heated under  $\text{N}_2$  at reflux for 30 min under an addition funnel filled with molecular sieves (4 Å). Compound **54** (0.005 g, 0.005 mmol) and compound **47T** (0.005 g, 0.005 mmol) were added in one portion and reflux was continued for 5 d. The reaction mixture was diluted with  $\text{CHCl}_3$  (20 mL), washed with water, dried over  $\text{MgSO}_4$ , and dried under high vacuum. The crude  $^1\text{H}$  NMR was taken in  $\text{DMSO}-d_6$  and only **54**, **47T**, and **47C** were observed.

**Acknowledgment.** We thank the University of Maryland and the NIH (GM61854) for generous financial support. We also thank the reviewers for their insights.

**Supporting Information Available:** Experimental procedures and characterization data for new compounds (**30**, **31**, **32**, and **56**), including CIF files, and selected  $^1\text{H}$  and  $^{13}\text{C}$  NMR spectra. This material is available free of charge via the Internet at <http://pubs.acs.org>.

JO051655R